

AperTO - Archivio Istituzionale Open Access dell'Università di Torino

Systemic and Targeted Delivery of Semaphorin 3A Inhibits Tumor Angiogenesis and Progression in Mouse Tumor Models

This is the author's manuscript

Original Citation:

Availability:

This version is available <http://hdl.handle.net/2318/111706> since

Published version:

DOI:10.1161/ATVBAHA.110.211920

Terms of use:

Open Access

Anyone can freely access the full text of works made available as "Open Access". Works made available under a Creative Commons license can be used according to the terms and conditions of said license. Use of all other works requires consent of the right holder (author or publisher) if not exempted from copyright protection by the applicable law.

(Article begins on next page)



UNIVERSITÀ DEGLI STUDI DI TORINO

This is an author version of the contribution published on:

Questa è la versione dell'autore dell'opera:

Arteriosclerosis Thrombosis and Vascular Biology, volume 31 issue 4, 2011, doi:

10.1161/ATVBAHA.110.211920

The definitive version is available at:

La versione definitiva è disponibile alla URL:

<http://atvb.ahajournals.org/content/31/4/741.long>

Systemic and Targeted Delivery of Semaphorin 3A Inhibits Tumor Angiogenesis and Progression in Mouse Tumor Models

Andrea Casazza, Xi Fu, Irja Johansson, Lorena Capparuccia, Fredrik Andersson, Alice Giustacchini, Mario Leonardo Squadrito, Mary Anna Venneri, Massimiliano Mazzone, Erik Larsson, Peter Carmeliet, Michele De Palma, Luigi Naldini, Luca Tamagnone, Charlotte Rolny

Author Affiliations

From the Institute for Cancer Research and Treatment, University of Turin School of Medicine, Candiolo, Italy (A.C., L.C., L.T., C.R.); Department of Genetics and Pathology, Rudbeck Laboratory, Uppsala University, Uppsala, Sweden (X.F., I.J., F.A., E.L., C.R.); Angiogenesis and Tumor Targeting Research Unit and San Raffaele-Telethon Institute for Gene Therapy, San Raffaele Scientific Institute, Milan, Italy (A.G., M.L.S., M.A.V., M.D.P., L.N.); Vita-Salute San Raffaele University, Milan, Italy (A.G., M.L.S., L.N.); Vesalius Research Center, Vesalius Research Center (VIB), Leuven, Belgium (M.M., P.C.); Vesalius Research Center, Katholieke Universiteit (KU) Leuven, Leuven, Belgium (M.M., P.C.).

Correspondence to Luca Tamagnone, Institute for Cancer Research and Treatment, University of Turin School of Medicine, Strada Prov. 142, 10060 Candiolo (TO), Italy. E-mail luca.tamagnone@ircc.it

Dr Casazza and Mr Fu contributed equally to this work, and Drs Tamagnone and Rolny contributed equally to this work.

ABSTRACT

Objective—The role of semaphorins in tumor progression is still poorly understood. In this study, we aimed at elucidating the regulatory role of semaphorin 3A (SEMA3A) in primary tumor growth and metastatic dissemination.

Methods and Results—We used 3 different experimental approaches in mouse tumor models: (1) overexpression of SEMA3A in tumor cells, (2) systemic expression of SEMA3A following liver gene transfer in mice, and (3) tumor-targeted release of SEMA3A using gene modified Tie2-expressing monocytes as delivery vehicles. In each of these experimental settings, SEMA3A efficiently inhibited tumor growth by inhibiting vessel function and increasing tumor hypoxia and necrosis, without promoting metastasis. We further show that the expression of the receptor neuropilin-1 in tumor cells is required for SEMA3A-dependent inhibition of tumor cell migration in vitro and metastatic spreading in vivo.

Conclusion—In sum, both systemic and tumor-targeted delivery of SEMA3A inhibits tumor angiogenesis and tumor growth in multiple mouse models; moreover, SEMA3A inhibits the metastatic spreading from primary tumors. These data support the rationale for further investigation of SEMA3A as an anticancer molecule.

Key Words: angiogenesis, molecular biology, pathology, receptors, vascular biology, metastasis, neuropilin, semaphorin, tumor

Semaphorins are a highly conserved family of molecules originally identified as axon guidance factors.^{1,2} Notably, over the past few years, distinct semaphorins have been implicated in additional biological processes, including angiogenesis, immune regulation, and cancer.^{3,4}

Semaphorin function is mediated by a family of plasma membrane receptors, the plexins.⁵ However, most secreted semaphorins (including semaphorin 3A [SEMA3A]) cannot bind to plexins directly; rather, they interact with plexin-associated coreceptors, namely neuropilin-1 (NP1) and neuropilin-2 (NP2).^{3,5} Interestingly, NPs also bind vascular endothelial growth factor family members and associate in complex with vascular endothelial growth factor receptors,⁶ playing a crucial role in angiogenesis beyond axon guidance.³ In particular, SEMA3A signaling is fully dependent on the receptor NP1, whereas little is known about the requirement of specific plexins in its receptor complex.

So far, SEMA3A has been reported to inhibit the growth of certain experimental tumors⁷ and to regulate endothelial cell migration and apoptosis *in vitro*,^{8,9} as well as arteriogenesis in the muscle,¹⁰ skin vessel permeability,¹¹ and tumor angiogenesis *in vivo*.¹² However, the functional significance of SEMA3A signaling as a molecular target to control tumor progression is still poorly understood. Generally, tumor blood vessels display a chaotic architecture that leads to impaired tumor perfusion, elevated tissue hypoxia, and substantial cell death. It has been shown that antiangiogenic treatments targeting vascular endothelial growth factor signaling can disrupt tumor blood vessels and increase tumor necrosis. However, these therapies, although they cause transient tumor shrinkage, also elicit a prometastatic program in the tumor cells that is driven by hypoxia.^{13,14} Therefore, strategies that concomitantly target endothelial cells and prevent tumor cell spreading are needed. Here, we show that systemic, as well as tumor-targeted, delivery of SEMA3A inhibits tumor growth in multiple mouse models. This is achieved through SEMA3A-mediated inhibition of blood vessel function, whereas metastatic dissemination is hindered via NP1-mediated signaling in tumor cells.

METHODS

Tumor Cell Lines

Tumor cell lines were grown in standard medium supplemented with L-glutamine and 10% fetal bovine serum (Sigma). 4T1 and 66cl4 spontaneous mouse mammary carcinoma cells were originally derived from a single spontaneous tumor arisen in a BALB/cfC3H mouse, isolated by 60 μ M 6-thioguanine *in vitro* selection, and kindly provided by Dr F. Miller (Michigan Cancer Foundation, Detroit, MI).¹⁵ MDA-MB-435 cells are undifferentiated tumor cells derived from either human mammary carcinoma or, as recently found, from human melanoma.¹⁶

Lentiviral Vectors

The LV constructs expressing green fluorescent protein (GFP) under different promoters: i.e. Tie2, phosphoglycerate kinase (PGK) and cytomegalovirus (CMV) were previously described.¹⁷ The Tie2-3A, PGK-3A, and CMV-3A LVs were generated by cloning the mouse Sema3A cDNA in place of GFP into the Tie2-GFP or PGK-GFP LV or human SEMA3A cDNA into the CVM-GFP LV, respectively. Concentrated vesicular stomatitis virus-G protein (VSV-G)-pseudotyped LV stocks were produced and titrated as described previously.¹⁸ Tumor cells were transduced by incubation with concentrated LVs for 8 to 12 hours in the presence of 8 μ g/mL polybrene.

SDS-PAGE and Western Immunoblotting

Cellular proteins were solubilized in 1% Triton X-100-containing extraction buffer plus inhibitors, as previously described.¹⁸ Equal amount of proteins were separated by SDS-PAGE, transferred to nitrocellulose membranes and probed with antibodies directed against myc-tag (9E10, Santa Cruz

Biotechnology), NP1 (R&D Systems), or β -actin (Santa Cruz Biotechnology), followed by detection using the appropriate secondary antibody and ECL system (Amersham).

Gene Knockdown

NP1 expression was stably knocked down in 4T1 cancer cells using a LV containing a gene-targeted short hairpin RNA against NP1 and a puromycin resistance cassette (Sigma Mission, NM_009152).

Cell Growth Assay

Tumor cells were plated in multiple 96-well dishes (Costar) at an initial density of 1×10^3 cells/well. After 24 hours of serum starvation, the cells were cultured in Dulbecco's modified Eagle's medium supplemented with L-glutamine and 1% fetal bovine serum for 1, 2, 3, and 4 days. Cells were fixed with 11% glutaraldehyde and then stained with 0.5% crystal violet in 20% methanol. The dye was eluted with 10% v/v glacial acetic acid, and the absorbance at 595 nm was determined by using a Titertek Multiskan reader.

Cell Migration Assay

Cell motility was assayed using Transwell chamber inserts (Costar, Cambridge, MA) with a porous polycarbonate membrane (8 μ mol/L pore size), as described previously.¹⁹ Briefly, the lower side of the filter was coated with 10 μ g/mL fibronectin. Approximately 1×10^5 cells were added in the upper chamber and allowed to migrate through the filter toward the lower chamber containing serum free medium (0.2% bovine serum albumin) with or without SEMA3A, in the presence of 15 μ g/mL purified anti-NP1 blocking antibody²⁰ or an unrelated antibody (anti-VSV-G). Cell migration was allowed for 16 to 18 hours; the cells adherent to the upper side of the filter were mechanically removed, whereas those migrated to the lower side were fixed with 11% glutaraldehyde and stained with crystal violet. The dye was solubilized in 10% acetic acid to measure absorbance at 595 nm in a microplate reader.

Mouse Tumor Models

Six- to 8-week-old CD1 athymic mice and Balb/c mice were purchased from Charles River Laboratory (Calco, Milan, Italy). FVB/Tie2-GFP transgenic mice were generated by LV-mediated transgenesis, as described.¹⁷ For tumorigenesis experiments, depending on the cancer cell line used, 2×10^6 MDA-MB-435, 1×10^6 66cl4, or 1×10^6 4T1 cells were injected subcutaneously into the flank or the mammary fat pad of anesthetized animals. Tumor size was measured externally using a caliper, and tumor volume was estimated using the following equation: $V = 4/3\pi \times (d/2)^2 \times D/2$, where d is the minor tumor axis and D is the major tumor axis. Mice were typically euthanized 3 weeks after tumor cell injection (unless otherwise indicated in the manuscript), and tumors weighted after dissection. Superficial pulmonary metastases were contrasted by black India-ink airways infusion, and counted on dissected lung lobes under a stereoscopic microscope. For orthotopic tumor cell injection, 1×10^6 4T1 or 1×10^6 4T1 66cl4 cells were resuspended in 40 μ L of phosphate-buffered saline and injected into the second mammary fat pad of anesthetized Balb/c mice. Mice were euthanized after 15 or 19 days, respectively, and tumor and lungs were analyzed as described above. For systemic delivery of SEMA3A in vivo, concentrated PGK-3A and control LVs were administered by tail vein injection in 6- to 8-week-old Balb/c mice, 2 weeks before subcutaneous tumor cell injection.

All animal procedures were performed according to protocols approved by the animal experimentation supervising boards of the University of Torino, Fondazione San Raffaele del Monte Tabor (Milan, Italy), and Uppsala University.

Experimental Metastasis Assays

4T1 cancer cells (2.5×10^5 cells) were injected in the lateral tail vein of CD1 athymic mice; the formation of metastatic colonies in the lungs was analyzed 8 days later by black India ink airways infusion, as described above. For short-term experiments evaluating the metastatic extravasation of fluorescent 4T1 cells, we labeled cancer cells in culture by a short incubation with 10 $\mu\text{mol/L}$ CFDA SE Vybrant cell tracker (Molecular probes) according to the manufacturer's instructions, before cell injection in the tail vein.²¹ Tumor cell colonization of lung tissue was analyzed 48 hours later in at least 5 pairs of lungs in each experimental group (10 independent microscopic fields/lung) using the Metamorph software.

Metastatic Cell Clonogenic Assays

These assays were performed as described previously.¹⁵ After euthanasia, the lungs, lymph nodes, brain and liver were removed from tumor-bearing mice, minced into pieces, and incubated with a cocktail containing 1.5 mg/mL collagenase type IV (Sigma) and 2 mg/mL dispase (Sigma) at 37°C. Tissue samples were then mechanically dispersed and passed through 19- and 25-gauge needles to form a single cell suspension, which was plated out in complete culture medium supplemented with 60 $\mu\text{mol/L}$ 6-thioguanine. After 10 to 12 days, growing colonies were fixed with methanol, stained with crystal violet, and counted under a dissection microscope.

Hematopoietic Stem/Progenitor Cell Transduction and Transplantation

Six-week-old female CD1 athymic, FVB, and FVB/Tie2-GFP and mice were killed with CO₂, and their bone marrow (BM) was harvested by flushing the femurs and the tibias. Lineage-negative cells enriched in hematopoietic stem/progenitor cells were isolated from BM cells using a cell purification kit (Stem Cell Technologies) and transduced by concentrated LVs, as described.^{22,23} Briefly, 10^6 cells/mL were transduced with a LV dose equivalent to 3 to 4 $\mu\text{g/mL}$ HIV p24 (for Tie2-Sema3A and PGK-Sema3A LVs) or 10^8 GFP transducing units/mL (for Tie2-GFP and PGK-GFP LVs) for 12 hours in serum-free StemSpan medium (Stem Cell Technologies) containing a cocktail of cytokines (interleukin-3 [10 ng/mL], interleukin-6 [20 ng/mL], SCF [100 ng/mL], and Fms-related tyrosine kinase 3 ligand [10 ng/mL], all from Serotec). After transduction, 10^6 cells were infused into the tail vein of lethally irradiated, 6-week-old female CD1 athymic mice (radiation doses: 975 cGy). Vector copy number in BM cells was measured by quantitative polymerase chain reaction of vector sequences at the end of the experiments, as described.²⁴ Colony forming cell assays were performed as described.^{22,23} The engraftment of hematopoietic stem/progenitor cells transduced with the Tie2-SEMA3A-myc LV was assessed in transplanted mice by anti-Tie2 and anti-myc immunostaining of circulating cells, using a BD FACSCanto (BD Bioscience) analyzer.

Hypoxia and Tumor Perfusion

Tumor hypoxia was detected 2 hours after injection of 60 mg/kg pimonidazole hydrochloride in tumor-bearing mice. Mice were then euthanized, and tumors were harvested. To detect the formation of pimonidazole adducts, tumor paraffin sections were immunostained with Hypoxyprobe-1-Mab1 (Hypoxyprobe kit, Chemicon) following the manufacturer's instructions. Blood vessel permeability was detected by intravenous injection of 0.05 mg of 70-kDa fluorescein isothiocyanate (FITC)-conjugated dextran or biotin-conjugated dextran (Molecular Probes) and of 0.05 mg of FITC-conjugated Tamato Lectin (Vector Laboratories) in tumor-bearing mice; this relatively small molecule extravasates readily from leaky tumor blood vessels.^{25,26} Ten minutes later, mice were perfused by intracardiac injection of saline and 2% paraformaldehyde (5 minutes) and the tumors harvested and frozen in OCT compound. Blood vessel permeability was analyzed by measuring the area of extravasated dextran. Blood vessel perfusion was analyzed by injecting

0.05 mg of nonpermeable high-molecular-weight tetramethylrhodamine-labeled dextran (2 MDa, Molecular Probes) in tumor-bearing mice, 10 minutes before tumor excision.²⁵ Tumors were then fixed in 4% paraformaldehyde for 2 hours and frozen in OCT compound for immunofluorescence analysis.

Histological Analysis

Tumors samples were frozen in OCT compound, cut in 10- μ m thick sections, and immunostained with the appropriate antibodies, directed to cleaved caspase-3 (5A1E, Cell Signaling), myc (9E10, Santa Cruz Biotechnology), CD31, CD11b (BD Biosciences), F4/80 (Serotec), NG2 (Millipore), LYVE-1 (R&D Systems), Tie2 (eBioSciences), α -smooth muscle actin (α -SMA)-FITC (Sigma), and cleaved caspase-3 (Cell Signaling). Streptavidin and all secondary antibodies were conjugated with Alexa Fluor 488 or Alexa Fluor 546 fluorochromes (Molecular Probes). Cell nuclei were labeled with 4',6-diamidino-2-phenylindole (Invitrogen Corp). Multiple independent fields from sections of at least 4 tumors for each experimental condition were analyzed by using a Leica DM IRBM microscope, a Nikon TE300 Eclipse inverted fluorescence microscope, or a LSM 510 META confocal microscope and quantified by ImageJ software.

Statistical Analyses

Throughout the study, graphs always show average values \pm standard deviation (SD) unless otherwise indicated. Statistical analyses were performed by unpaired Student *t* test or 2-way ANOVA, as indicated. Stars in the graphs indicate significance, as detailed in the figure legends. Differences were considered statistically significant at $P < 0.05$.

RESULTS

SEMA3A Inhibits Tumor Growth and Metastatic Progression

To investigate the role of SEMA3A in tumor cell behavior and progression, we transduced 3 different tumor cell lines (4T1 and 66cl4 mammary carcinoma and MDA-MB-435 melanoma cells) with a SEMA3A-expressing LV, and obtained 3A⁺ cells. Control cells were generated by transducing the aforementioned tumor cell lines with a LV lacking the SEMA3A cDNA (referred to as empty vector [EV] cells). We confirmed SEMA3A expression in transduced cells by Western blotting (Figure 1A and Supplemental Figure IA, available online at <http://atvb.ahajournals.org>). Notably, in addition to endothelial cells, the SEMA3A receptor NP1 is expressed in most tumor cells, including those used in our study (see Supplemental Figure II). Although it has been reported that SEMA3A can inhibit the growth of certain tumor cell lines in an NP1-dependent manner,⁷ in our experiments, SEMA3A overexpression did not affect tumor cell proliferation, even on serum deprivation (Figure 1B and 1C and Supplemental Figure IB). However, SEMA3A strongly inhibited tumor cell migration via NP1, as demonstrated by using an NP1-blocking antibody (Figure 1D and 1E and Supplemental Figure IC).

Despite the fact that SEMA3A autocrine loop in tumor cells did not affect cell proliferation or survival in vitro, when these engineered cells were implanted in vivo, we found that tumor growth was strongly inhibited by SEMA3A expression (Figure 1F and 1G and Supplemental Figure ID and IH). Moreover, 3A⁺ tumor-bearing mice displayed fewer spontaneous lung metastatic nodules compared with controls (Figure 1H and Supplemental Figure IE). Because SEMA3A proved to actively inhibit tumor cell migration in vitro, we aimed at better understanding the role of SEMA3A in controlling metastatic dissemination. We then introduced fluorescently labeled 4T1-EV and 4T1-3A⁺ tumor cells in the tail vein, and 48 hours postinjection, we scored the number of tumor cells colonizing the lungs. Notably, SEMA3A expression strongly reduced the number of tumor cells that

successfully extravasated and colonized the lungs (Figure 1I), indicating that this semaphorin can directly regulate metastasis formation.

4T1 tumor cells are known to spread to additional metastatic sites beyond the lungs, such as lymph nodes, liver and brain, whereas 66cl4 mainly spread via the lymphatic route to the lungs.¹⁵ To investigate whether SEMA3A also affects metastatic dissemination to other distant organs, we injected 4T1 and 66cl4 control-EV or 3A⁺ cells in the mammary fat pad of wild-type female mice to produce orthotopic mammary tumors. After 15 days, we euthanized the mice and harvested the liver, brain, lungs, draining lymph nodes and blood. Dissociated cells from the different organs were then subjected to clonogenic assays in culture, in the presence of the selection drug 6-thioguanine, for which both 4T1 and 66cl4 cells carry the resistance gene.^{15,27} In line with previous reports,¹⁵ 66cl4-EV tumor cells formed several colonies from lymph nodes and few colonies from the lung (Figure 1J), but none from liver, brain, or blood. On the other hand, 4T1-EV tumor cells readily formed tumor cell colonies from the lung and, to a lesser extent, from liver, lymph nodes, and brain (Figure 1K). SEMA3A expression in 66cl4 and 4T1 tumor cells significantly decreased the number of colony-forming metastatic cells in each of the analyzed organs (Figure 1J and 1K). Interestingly, although the number of colonies derived from blood was low, it was also reduced in 4T1–3A⁺tumor-bearing mice (data not shown).

SEMA3A Inhibits Tumor Growth and Metastasis Via Independent Signaling in Stromal and Cancer Cells

Because SEMA3A has been shown previously to regulate angiogenesis, we aimed at dissecting the functional relevance of SEMA3A signaling in cancer cells and in the tumor microenvironment. To this end, we knocked down the expression of the obligate SEMA3A-receptor NP1 in 4T1-EV and 4T1–3A⁺ tumor cells by RNA interference-mediated technology and injected the resultant cells subcutaneously in mice (Figure 2A). Notably, NP1 gene knockdown did not alter the growth of 4T1-EV or 4T1–3A⁺ cells in culture (not shown), nor that of the tumors formed in vivo (Figure 2B), suggesting that SEMA3A-induced inhibition of tumor growth is independent from NP1 expression by tumor cells. Moreover, although NP1 gene knockdown did not affect the metastatic dissemination of control 4T1-EV cells, it led to a significant increase of lung metastasis formed by 4T1–3A⁺ cells (Figure 2C). These data suggest that SEMA3A-mediated suppression of metastatic dissemination depends on NP1-mediated signaling in cancer cells.

SEMA3A Inhibits Tumor Growth Via Paracrine Effects on Tumor Vasculature

The findings above strongly suggested that SEMA3A-dependent inhibition of tumor growth seen in our experiments was due to a paracrine effect in the tumor microenvironment. To study the implicated mechanisms, we therefore analyzed tissue sections derived from primary tumors. We found that 4T1- and 66cl4–3A⁺tumors displayed 25% increased necrotic areas compared with controls (Supplemental Figure III). Moreover, SEMA3A⁺ tumors displayed higher proportions of the apoptotic marker cleaved caspase-3 in tumor and endothelial cells compared with controls (Figure 3A, Supplemental Figure IF, and data not shown). Consistently, SEMA3A expression by tumor cells was associated with reduced vascular area and vessel density (Figure 3B, Supplemental Figure IG, and data not shown). To further investigate whether SEMA3A had a direct effect on the tumor endothelium, SEMA3A-expressing MDA-MB-435 tumor cells were cocultured with primary human endothelial cells in vitro. Staining for CD31 and cleaved caspase-3 revealed that SEMA3A induced endothelial cell apoptosis (Supplemental Figure IV). These data indicate direct proapoptotic effects of SEMA3A on endothelial cells.

Endothelial cell survival often correlates with the extent of pericyte coverage of endothelial cells in blood vessels.²⁸ Double staining for CD31 and the pericyte markers α -SMA and NG2 indicated that SEMA3A expression by tumor cells impaired pericyte coverage of tumor blood vessels (Figure 3C). Because Sema3A reduced 66cl4 tumor cell spreading to lungs and lymphatics, we investigated whether SEMA3A-expressing tumors displayed any defects in lymphangiogenesis. To this end, we stained tumor sections with antibodies against LYVE-1, which labels lymphatic vessels and a subset of F4/80⁺ tumor-associated macrophages.²⁹ Interestingly, 3A⁺ tumors displayed fewer lymphatic vessels, as shown by the reduced relative area of LYVE-1⁺F4/80⁻CD31⁻ vascular structures (Supplemental Figure V).

Systemic Delivery of SEMA3A Efficiently Inhibits Tumor Progression

Once a tumor has disseminated to distant organs, the local delivery of tumor suppressor molecules may not be a therapeutically feasible strategy. Thus, we assessed the potential antitumor activity of SEMA3A in a model of systemic delivery in vivo. We used a previously validated strategy to achieve systemic expression of secreted factors in tumor-recipient mice.³⁰ On injection in the venous circulation, LVs preferentially transduce the liver and the spleen, where they establish a stable source of the transgene product.³¹ By this approach, we generated mice stably expressing SEMA3A (here referred to as s-SEMA3A mice), or control mice (s-EV mice). SEMA3A expression was detected in the liver by immunohistochemistry (Supplemental Figure VI) and in blood samples by ELISA (estimated levels: 95% confidence interval=77.06 to 94.58 ng/mL). SEMA3A-treated mice did not display histological abnormalities or increased apoptosis in the liver (data not shown), nor did they show any significant change in blood lymphocyte or erythrocyte counts and hemoglobin levels (data not shown).

4T1 or 66cl4 metastatic mammary carcinoma cells were then transplanted subcutaneously in syngeneic s-Sema3A and control mice. Analogously to what was observed on SEMA3A overexpression in cancer cells, the systemic expression of SEMA3A efficiently inhibited 4T1 and 66cl4 tumor growth (Figure 4A) and metastatic dissemination in mice (Figure 4B). Notably (and consistent with data shown in Figure 1D and 1E), 4T1 and 66cl4 tumor cell migration in vitro was strongly inhibited by exogenous SEMA3A (Figure 4C). To further elucidate the antimetastatic effect of SEMA3A, systemic delivery of SEMA3A was compared with its overexpression in 4T1–3A⁺ cells, in a model of experimental lung metastasis that is independent of the growth of primary tumors. Both systemic and tumor cell-based expression of SEMA3A impaired the formation of lung metastatic colonies by 4T1 cells systemically injected in the mouse circulation (Figure 4D), further supporting the hypothesis that SEMA3A has a direct effect on tumor cell extravasation and lung colonization.

We then investigated whether the systemic delivery of SEMA3A produced the same effects on tumor vasculature and apoptosis in primary tumors as its overexpression in tumor cells. CD31 staining of tumor sections revealed that the relative vessel area was reduced in 4T1 and 66cl4 tumors grown in s-SEMA3A mice compared with those in control s-EV mice (Figure 4E). Consistently, the systemic delivery of SEMA3A enhanced tumor cell and blood vessel apoptosis (visualized by staining for cleaved caspase-3; Figure 4F) and reduced the number of tumor blood vessels covered with NG2- or α -SMA-expressing pericytes (Figure 5A). A reduced pericyte coverage often correlates with increased vessel permeability and poor vessel functionality,^{32,33} which may lead to increased tumor hypoxia, conditions that were previously found to favor tumor cell intravasation and to fuel the metastatic spreading.^{13,14,34} We then measured tumor blood vessel permeability by systemic injection of the readily diffusible 70-kDa FITC-conjugated dextran in tumor-bearing mice. Notably, tumors grown in s-SEMA3A mice displayed increased extravasated dextran (Figure 5B). Moreover, these tumors displayed increased tissue

hypoxia, as revealed by pimonidazole staining (Figure 5C). These data suggest that systemic expression of SEMA3A, though promoting a prometastatic tumor microenvironment (enhanced hypoxia and vascular leakiness), efficiently inhibits metastatic dissemination of tumor cells by exerting direct effects on tumor cells.

Tumor-Targeted Delivery of SEMA3A by TIE2-Expressing Monocytes Inhibits Tumor Progression

A subset of circulating and tumor-infiltrating proangiogenic monocytes/macrophages, which are characterized by the expression of the angiopoietin receptor Tie2 (Tie2-expressing monocytes [TEMs]), were recently exploited to deliver interferon- α to the tumor site.³⁵ These cells are derived from the bone marrow and can be used as cellular vehicles to achieve targeted delivery of inhibitory molecules to tumors, without generating high systemic blood concentrations of the secreted factor.³⁶ To accomplish TEM-mediated delivery of SEMA3A to tumors, we produced LVs expressing the murine SEMA3A cDNA under the control of promoter/enhancer sequences of the *Tie2* gene (Tie2-3A LV). Consistent with the notion that Tie2 is highly expressed in endothelial cells, the Tie2-3A LV expressed SEMA3A efficiently in brain endothelial cells but not in embryonic kidney HEK-293T cells in vitro (see Supplemental Figure VIIA).

Hematopoietic stem/progenitor cells obtained from the BM of FVB-Tie2-GFP transgenic mice³⁷ or FVB-WT mice were then transduced with the Tie2-3A LV and transplanted into lethally irradiated mice, to obtain mice with TEM-specific expression of m-SEMA3A (Tie2-SEMA3A mice; see schematic procedure in Supplemental Figure VIIB). Moreover, mice transplanted with BM cells transduced with Tie2-EV LVs were used as controls. Tie2-SEMA3A mice were reconstituted long-term by SEMA3A gene-modified BM cells and did not show any obvious signs of toxicity (data not shown).

Six weeks after hematopoietic stem/progenitor cell transplantation, 66cl4 mammary carcinoma cells were injected subcutaneously in both Tie2-3A and control mice to study tumor development. At the end of the experiments (6 weeks after tumor cell injection), we found that both primary tumor weight (Figure 6A) and metastatic spreading (Figure 6B) were reduced in Tie2-3A mice as compared with the controls. Notably, Tie2-Sema3A expression did not affect the number of circulating TEMs as estimated by fluorescence-activated cell sorting analysis of Tie2⁺CD115⁺ cells in the peripheral blood of Tie2-3A and Tie2-EV mice (1.02 \pm 0.39% versus 1.26 \pm 0.45% of total leukocytes, respectively; $P=0.69$; $n=6$). Moreover we found blood vessel-associated Tie2⁺ cells^{17,29} positive for SEMA3A expression (Figure 6C).

Immunostaining of tumor sections revealed that TEM-mediated SEMA3A delivery phenocopied the vascular changes observed on systemic delivery of SEMA3A. In particular, CD31 immunostaining indicated that tumors grown in Tie2-Sema3A mice had reduced relative blood vessel area (Figure 6D). Moreover, SEMA3A greatly impaired vessel functionality, as revealed by labeling perfused blood vessels with high-molecular-weight (2 MDa) TRITC-conjugated dextran injected in the circulation of tumor-bearing mice (Figure 6E). Consistent with the data observed in mice that received systemic SEMA3A, pericyte coverage of tumor vessels in Tie2-Sema3A mice was reduced (Figure 6F). Moreover, double staining for cleaved caspase-3 and CD31 showed that Tie2-Sema3A tumors contained a significantly increased fraction of apoptotic endothelial cells compared with controls (Figure 6G). The reduced blood vessel functionality in tumors grown in Tie2-Sema3A mice translated in an increased tumor hypoxia, as assessed by pimonidazole staining (Figure 6H). These data indicate that TEM-mediated delivery of SEMA3A can impair blood vessel formation and functionality, as well as the growth of primary tumors and their metastatic dissemination to the lungs.

DISCUSSION

Solid tumors cannot grow or spread without the formation of new blood vessels; this finding has driven several studies in the last decades aimed to find antiangiogenic therapeutic strategies. In this work, we have investigated the role of SEMA3A in tumor angiogenesis, tumor growth and metastatic dissemination using 3 different delivery strategies: (1) tumor cell-based gene transfer, (2) systemic expression of SEMA3A in mice, and (3) tumor macrophage-mediated local delivery in tumors. Although it has been reported that an autocrine loop of SEMA3A may inhibit the growth of tumor cells expressing high levels of NP1,⁷ we did not observe this effect in various tumor cell models analyzed in this study. However, SEMA3A did inhibit tumor cell migration in an NP1-dependent manner.

Recent studies have emphasized that tumor growth and metastatic dissemination is regulated not only by blood vessel density but, most importantly, by blood vessel functionality.^{34,38} The tumor vasculature typically displays a high-density irregular network, and it is often characterized by inadequate coverage by mural cells; this inadequate coverage has also been implicated in the metastatic spreading.³⁹ An abnormal tumor vasculature is generally poorly perfused, which results in enhanced tumor cell apoptosis, necrosis and hypoxia. Therapeutic approaches aimed at further reducing vessel perfusion usually impair tumor growth; this may also affect metastasis formation as a secondary effect to the reduction of primary tumor burden. However, it has recently been shown that tumor shrinkage achieved by antiangiogenic drugs interfering with vascular endothelial growth factor signaling may instead be associated with increased metastatic spreading.^{13,14} Although the molecular mechanisms responsible for these processes are currently unknown, it has been proposed that hypoxic tissues switch on a transcriptional “escape” program, leading to increased cancer cell invasiveness.⁴⁰

In our study, we demonstrated that systemic or local expression of SEMA3A impairs tumor angiogenesis and reduces the number of pericyte-coated vessels. This resulted in decreased vessel perfusion and increased hypoxia, in association with tissue apoptosis and necrosis; thus, SEMA3A-treated tumors were significantly smaller than controls. Importantly, although hypoxic and apoptotic, these tumors did not become invasive and metastatic, suggesting that SEMA3A could concomitantly interfere with cancer cell behavior. In fact, we showed that, independently from its paracrine activity on tumor vasculature, SEMA3A inhibits the metastatic dissemination by acting directly on cancer cell migration in NP1-dependent manner. This was demonstrated by distinct experimental strategies: (1) NP1-neutralizing antibodies abrogated SEMA3A-dependent inhibition of tumor cell migration, and (2) NP1 expression knockdown in cancer cells prevented SEMA3A-mediated inhibition of metastatic dissemination *in vivo*.

Importantly, the potency of the antiangiogenic activity of SEMA3A will depend on the active concentration that is reached within the tumor site and tumor vessels and on its ability to counterbalance the effect of proangiogenic factors usually present in the tumor microenvironment. For instance, the local delivery of SEMA3A in a transgenic oncogene-driven model of pancreatic islet cell carcinogenesis resulted in a mild and transient antiangiogenic effect, which eventually subsided into vessel “normalization” rather than further disruption.¹² This resulted in a moderate SEMA3A-dependent inhibition of tumor growth that was sufficient to prolong overall survival by delaying the occurrence of lethal hyperinsulinemia; however, time persistence of tumor suppression and potential metastatic progression were not investigated. In our present study, by exploiting multiple experimental tumor models and delivery routes based on LV-mediated gene transfer, we demonstrated that SEMA3A is a strong antiangiogenic factor novel in its kind, because it can impair tumor growth and prevent metastatic dissemination. In our experiments, the majority of vessels in SEMA3A-treated tumors were severely disrupted compared with controls, indicating a persistent inhibitory activity by the semaphorin, which overpowered local proangiogenic factors and resulted in sustained tumor suppression during the entire experiment. Moreover, we showed that

the metastatic spreading was not increased in presence of SEMA3A, because this versatile antiangiogenic factor also directly inhibited cancer cell migration.

In conclusion, our work provides proof of concept, in multiple preclinical models, that the antiangiogenic activity of SEMA3A may be exploited to effectively inhibit tumor growth and metastatic progression.

Sources of Funding

This work was supported by a grant from Italian Association for Cancer Research and from Regione Piemonte (to L.T.), a grant from the Italian Association for Cancer Research (to L.N.), a European Research Council (ERC) Starting Grant (to M.D.P.), Swedish Cancer Foundation Project CAN 2008/980, Marie Curie Re-Integration Grant Contract MERG-CT-2007-046454, and an Åke Wibergs Grant (to C.R.). A.C. was supported by an Italian Foundation for Cancer Research (FIRC) fellowship.

Disclosures

None.

Acknowledgments

We thank L. Palmas, S. Giove, and L. Fontani for skilful technical assistance. Anti-NP1 antibodies were generously provided by A. Kolodkin (Johns Hopkins University, Baltimore, MD).

REFERENCES

1. Luo Y, Raible D, Raper JA. Collapsin: a protein in brain that induces the collapse and paralysis of neuronal growth cones. *Cell*. 1993;75:217–227.
2. Kolodkin AL, Matthes DJ, Goodman CS. The semaphorin genes encode a family of transmembrane and secreted growth cone guidance molecules. *Cell*. 1993;75:1389–1399.
3. Neufeld G, Shraga-Heled N, Lange T, Guttmann-Raviv N, Herzog Y, Kessler O. Semaphorins in cancer. *Front Biosci*. 2005;10:751–760.
4. Capparuccia L, Tamagnone L. Semaphorin signaling in cancer cells and in cells of the tumor microenvironment: two sides of a coin. *J Cell Sci*. 2009;122:1723–1736.
5. Tamagnone L, Artigiani S, Chen H, He Z, Ming GI, Song H, Chedotal A, Winberg ML, Goodman CS, Poo M, Tessier-Lavigne M, Comoglio PM. Plexins are a large family of receptors for transmembrane, secreted, and GPI-anchored semaphorins in vertebrates. *Cell*. 1999;99:71–80.
6. Soker S, Miao HQ, Nomi M, Takashima S, Klagsbrun M. VEGF165 mediates formation of complexes containing VEGFR-2 and neuropilin-1 that enhance VEGF165-receptor binding. *J Cell Biochem*. 2002;85:357–368.
7. Kigel B, Varshavsky A, Kessler O, Neufeld G. Successful inhibition of tumor development by specific class-3 semaphorins is associated with expression of appropriate semaphorin receptors by tumor cells. *PLoS One*. 2008;3:e3287.
8. Miao HQ, Soker S, Feiner L, Alonso JL, Raper JA, Klagsbrun M. Neuropilin-1 mediates collapsin-1/semaphorin III inhibition of endothelial cell motility: functional competition of collapsin-1 and vascular endothelial growth factor-165. *J Cell Biol*. 1999;146:233–242.
9. Guttmann-Raviv N, Shraga-Heled N, Varshavsky A, Guimaraes-Sternberg C, Kessler O, Neufeld G. Semaphorin-3A and semaphorin-3F work together to repel endothelial cells and to inhibit their survival by induction of apoptosis. *J Biol Chem*. 2007;282:26294–26305.

10. Zacchigna S, Pattarini L, Zentilin L, Moimas S, Carrer A, Sinigaglia M, Arsic N, Tafuro S, Sinagra G, Giacca M. Bone marrow cells recruited through the neuropilin-1 receptor promote arterial formation at the sites of adult neoangiogenesis in mice. *J Clin Invest.* 2008;118:2062–2075.
11. Acevedo LM, Barillas S, Weis SM, Gothert JR, Cheresh DA. Semaphorin 3A suppresses VEGF-mediated angiogenesis yet acts as a vascular permeability factor. *Blood.* 2008;111:2674–2680.
12. Maione F, Molla F, Meda C, Latini R, Zentilin L, Giacca M, Seano G, Serini G, Bussolino F, Giraudo E. Semaphorin 3a is an endogenous angiogenesis inhibitor that blocks tumor growth and normalizes tumor vasculature in transgenic mouse models. *J Clin Invest.* 2009;119:3356–3372.
13. Ebos JM, Lee CR, Cruz-Munoz W, Bjarnason GA, Christensen JG, Kerbel RS. Accelerated metastasis after short-term treatment with a potent inhibitor of tumor angiogenesis. *Cancer Cell.* 2009;15:232–239.
14. Paez-Ribes M, Allen E, Hudock J, Takeda T, Okuyama H, Vinals F, Inoue M, Bergers G, Hanahan D, Casanovas O. Antiangiogenic therapy elicits malignant progression of tumors to increased local invasion and distant metastasis. *Cancer Cell.* 2009;15:220–231.
15. Aslakson CJ, Miller FR. Selective events in the metastatic process defined by analysis of the sequential dissemination of subpopulations of a mouse mammary tumor. *Cancer Res.* 1992;52:1399–1405.
16. Rae JM, Creighton CJ, Meck JM, Haddad BR, Johnson MD. MDA-MB-435 cells are derived from m14 melanoma cells: a loss for breast cancer, but a boon for melanoma research. *Breast Cancer Res Treat.* 2007;104:13–19.
17. De Palma M, Venneri MA, Galli R, Sergi L, Politi LS, Sampaolesi M, Naldini L. Tie2 identifies a hematopoietic lineage of proangiogenic monocytes required for tumor vessel formation and a mesenchymal population of pericyte progenitors. *Cancer Cell.* 2005;8:211–226.
18. Follenzi A, Naldini L. HIV-based vectors: preparation and use. *Methods Mol Med.* 2002;69:259–274.
19. Barberis D, Artigiani S, Casazza A, Corso S, Giordano S, Love CA, Jones EY, Comoglio PM, Tamagnone L. Plexin signaling hampers integrin-based adhesion, leading to rho-kinase independent cell rounding, and inhibiting lamellipodia extension and cell motility. *FASEB J.* 2004;18:592–594.
20. Kolodkin AL, LeVengood DV, Rowe EG, Tai YT, Giger RJ, Ginty DD. Neuropilin is a semaphorin III receptor. *Cell.* 1997;90:753–762.
21. Casazza A, Finisguerra V, Capparuccia L, Camperi A, Swiercz JM, Rizzolio S, Rolny C, Christensen C, Bertotti A, Sarotto I, Risio M, Trusolino L, Weitz J, Schneider M, Mazzone M, Comoglio PM, Tamagnone L. Sema3E-Plexin D1 signaling drives human cancer cell invasiveness and metastatic spreading in mice. *J Clin Invest.* 2010;120:2684–2698.
22. De Palma M, Naldini L. Transduction of a gene expression cassette using advanced generation lentiviral vectors. *Methods Enzymol.* 2002;346:514–529.
23. De Palma M, Venneri MA, Naldini L. In vivo targeting of tumor endothelial cells by systemic delivery of lentiviral vectors. *Hum Gene Ther.* 2003;14:1193–1206.
24. De Palma M, Montini E, Santoni de Sio FR, Benedicenti F, Gentile A, Medico E, Naldini L. Promoter trapping reveals significant differences in integration site selection between MLV and HIV vectors in primary hematopoietic cells. *Blood.* 2005;105:2307–2315.
25. Dreher MR, Liu W, Michelich CR, Dewhirst MW, Yuan F, Chilkoti A. Tumor vascular permeability, accumulation, and penetration of macromolecular drug carriers. *J Natl Cancer Inst.* 2006;98:335–344.
26. Criscuoli ML, Nguyen M, Eliceiri BP. Tumor metastasis but not tumor growth is dependent on src-mediated vascular permeability. *Blood.* 2005;105:1508–1514.

27. Miller BE, Delmonico L, Vistisen K, Miller FR. Use of tumor lines with selectable markers in assessing the effect on experimental metastases of combination chemotherapy with alkylating agents. *Clin Exp Metastasis*. 1998;16:480–488.
28. Bergers G, Song S. The role of pericytes in blood-vessel formation and maintenance. *Neuro-oncol*. 2005;7:452–464.
29. Pucci F, Venneri MA, Biziato D, Nonis A, Moi D, Sica A, Di Serio C, Naldini L, De Palma M. A distinguishing gene signature shared by tumor-infiltrating Tie2-expressing monocytes, blood “resident” monocytes and embryonic macrophages suggests common functions and developmental relationships. *Blood*. 2009;114:901–914.
30. Brown BD, Sitia G, Annoni A, Hauben E, Sergi LS, Zingale A, Roncarolo MG, Guidotti LG, Naldini L. In vivo administration of lentiviral vectors triggers a type I interferon response that restricts hepatocyte gene transfer and promotes vector clearance. *Blood*. 2007;109:2797–2805.
31. Brown BD, Venneri MA, Zingale A, Sergi L, Naldini L. Endogenous microRNA regulation suppresses transgene expression in hematopoietic lineages and enables stable gene transfer. *Nat Med*. 2006;12:585–591.
32. McDonald DM, Choyke PL. Imaging of angiogenesis: from microscope to clinic. *Nat Med*. 2003;9:713–725.
33. Jain RK. Molecular regulation of vessel maturation. *Nat Med*. 2003;9:685–693.
34. Mazzone M, Dettori D, Leite de Oliveira R, Loges S, Schmidt T, Jonckx B, Tian YM, Lanahan AA, Pollard P, Ruiz de Almodovar C, De Smet F, Vinckier S, Aragonés J, Debackere K, Lutun A, Wyns S, Jordan B, Pisacane A, Gallez B, Lampugnani MG, Dejana E, Simons M, Ratcliffe P, Maxwell P, Carmeliet P. Heterozygous deficiency of *phd2* restores tumor oxygenation and inhibits metastasis via endothelial normalization. *Cell*. 2009;136:839–851.
35. De Palma M, Mazziere R, Politi LS, Pucci F, Zonari E, Sitia G, Mazzoleni S, Moi D, Venneri MA, Indraccolo S, Falini A, Guidotti LG, Galli R, Naldini L. Tumor-targeted interferon- α delivery by Tie2-expressing monocytes inhibits tumor growth and metastasis. *Cancer Cell*. 2008;14:299–311.
36. De Palma M, Naldini L. Tie2-expressing monocytes (TEMs): novel targets and vehicles of anticancer therapy? *Biochim Biophys Acta*. 2009;1796:5–10.
37. De Palma M, Venneri MA, Roca C, Naldini L. Targeting exogenous genes to tumor angiogenesis by transplantation of genetically modified hematopoietic stem cells. *Nat Med*. 2003;9:789–795.
38. Stockmann C, Doedens A, Weidemann A, Zhang N, Takeda N, Greenberg JI, Cheresh DA, Johnson RS. Deletion of vascular endothelial growth factor in myeloid cells accelerates tumorigenesis. *Nature*. 2008;456:814–818.
39. Xian X, Hakansson J, Stahlberg A, Lindblom P, Betsholtz C, Gerhardt H, Semb H. Pericytes limit tumor cell metastasis. *J Clin Invest*. 2006;116:642–651.
40. Michieli P, Mazzone M, Basilico C, Cavassa S, Sottile A, Naldini L, Comoglio PM. Targeting the tumor and its microenvironment by a dual-function decoy met receptor. *Cancer Cell*. 2004;6:61–73.
41. Aslakson CJ, Rak JW, Miller BE, Miller FR. Differential influence of organ site on three subpopulations of a single mouse mammary tumor at two distinct steps in metastasis. *Int J Cancer*. 1991;47:466–472.

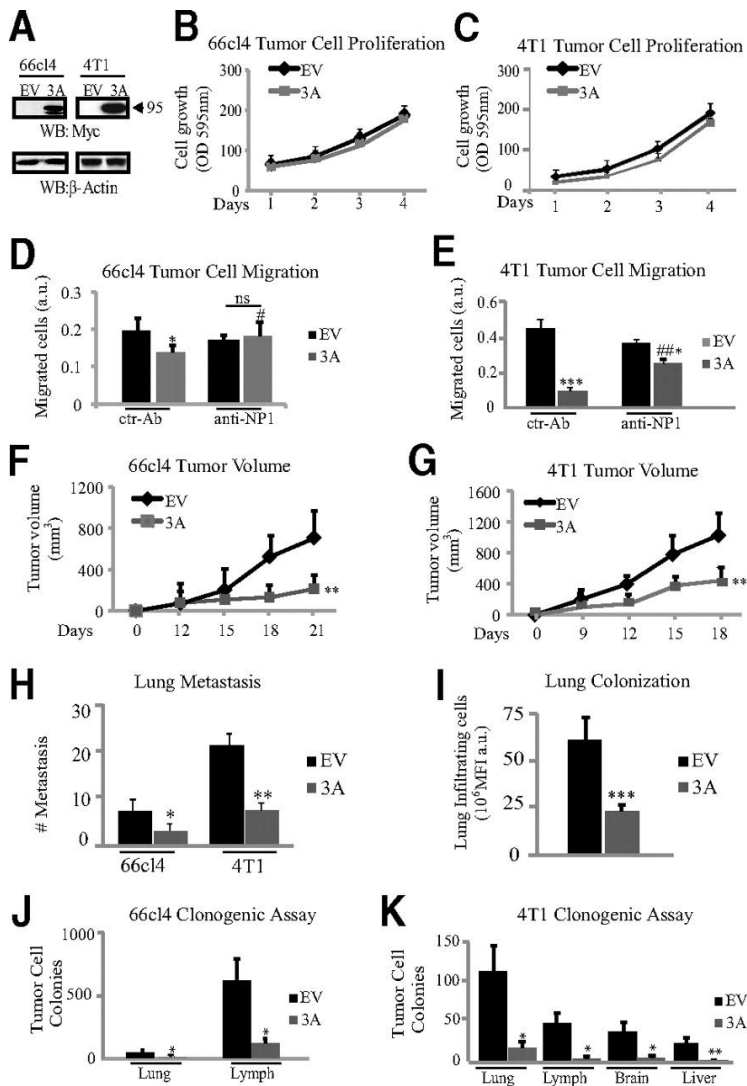


Figure 1.

Tumor growth is inhibited by cell-based therapy with SEMA3A. A, Western blotting (WB) analysis revealing the expression of myc-tagged SEMA3A (95 kDa) in protein lysates of LV-transduced 66cl4 and 4T1 tumor cells. Control cells were transduced with an EV. B and C, SEMA3A-expressing and tumor cells (66cl4 and 4T1, as indicated) proliferate in culture at comparable rates, in low-serum conditions (1% fetal bovine serum). Cell growth was quantified by staining with crystal violet (see Methods for details). D and E: Cancer cell migration was analyzed by using Transwell inserts (see Methods). EV-control and SEMA3A⁺ tumor cells were allowed to spontaneously migrate through a semipermeable membrane in the presence of either NP1-blocking or unrelated control antibodies. The migration of 66cl4-3A⁺ and 4T1-3A⁺ cells was significantly reduced compared with 66cl4-EV and 4T1-EV cells. NP1-neutralizing antibodies blunted the inhibitory effect of SEMA3A for both cancer cells. Asterisks (*) indicate statistically significant differences compared with controls (****P*<0.001, **P*<0.05). Hatch marks (#) indicate significance compared with 3A⁺ tumor cells treated with control antibody (##*P*<0.01, #*P*<0.05). Each experiment was repeated at least twice. F to H, SEMA3A-expressing and EV-control-transduced tumor cells described above were transplanted subcutaneously into athymic mice. SEMA3A expression significantly reduced tumor growth (F and G) and metastatic dissemination to the lungs (H) in both tumor models (*n*=6; ***P*<0.01, **P*<0.05, with 2-way ANOVA and the Student *t* test). I, Fluorescence-labeled 4T1-3A⁺ or 4T1-EV cells were injected intravenously in mice, and their ability to infiltrate and colonize the lungs was scored after 48 hours (for details, see Methods; *n*=5; ****P*<0.001). J and K, 66cl4-EV and 3A⁺ and 4T1-EV and 3A⁺ cells were injected into the mammary fat pad to form primary orthotopic tumors. After euthanization, liver, brain, lungs, and drained lymph nodes were excised. Metastatic cells present in the different organs were subjected to clonogenic assay in culture to attain their quantification, as previously shown.¹⁵ Consistent with previous reports, 66cl4 cells primarily colonized the lung via the lymphatic system,^{15,41} and metastatic cells could not be isolated from liver and brain. SEMA3A expression reduced the number of metastatic cells in all the distant organs, for both tumor models (*n*=8; ***P*<0.01, **P*<0.05).

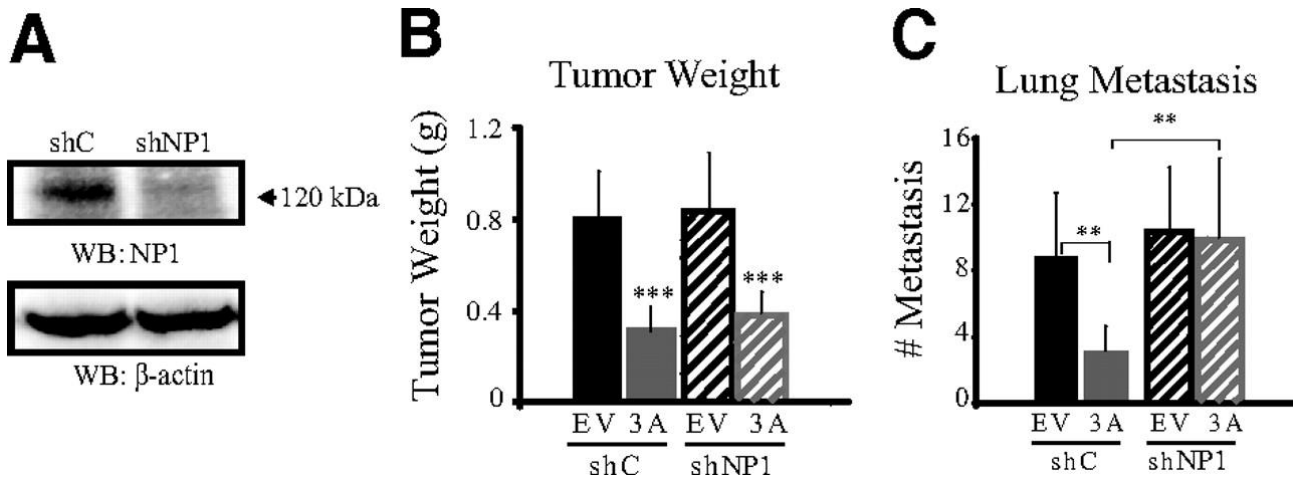


Figure 2.

Sema3A-NP1 signaling in cancer cells is not responsible for tumor suppression but restrains the metastatic spreading. A, Western blotting analysis demonstrating RNA interference-mediated knockdown of NP1 expression in 4T1 cancer cells, by means of a gene-targeted short hairpin RNA (shNP1); a non-targeting construct was used as control (shC). B, 4T1-EV or 4T1-3A⁺ cells were transplanted subcutaneously in athymic mice; tumor weight and number of superficial lung metastasis were scored 22 days after injection. NP1 knockdown did not affect tumor growth of 4T1-EV or 4T1-3A⁺ tumors (n=6; ****P*<0.001). C, The presence of macrometastasis was assessed in the lungs of the tumor-bearing mice described above. NP1-depleted cells were insensitive to SEMA3A-mediated inhibition of metastatic spreading (n=6; ***P*<0.02).

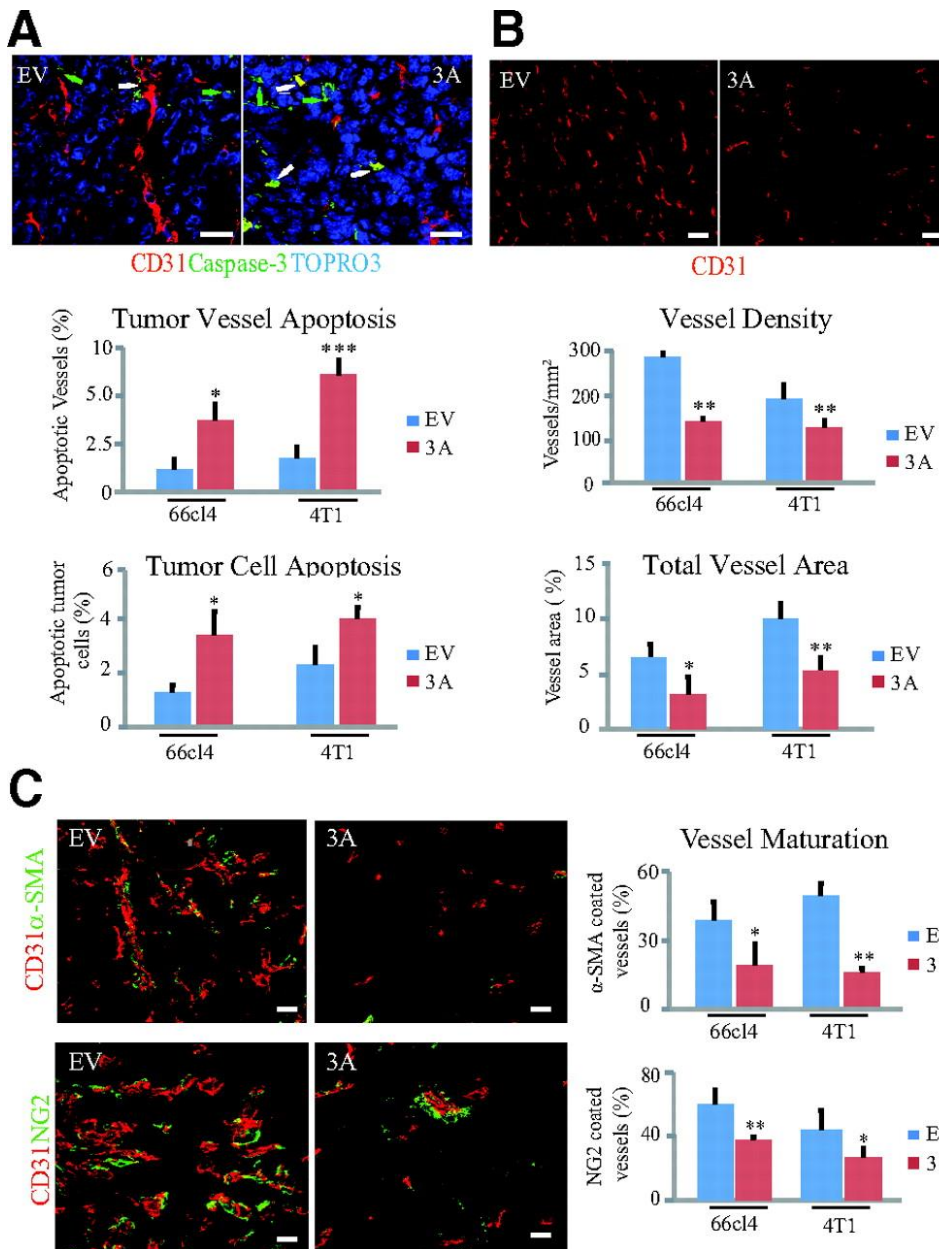


Figure 3.

SEMA3A inhibits tumor angiogenesis. A, 66c14-EV and -3A⁺ and 4T1-EV and -3A⁺ tumor sections were subjected to immunostaining for activated-caspase3 to detect apoptotic cells (in green), CD31 marker was stained to identify endothelial cells (red), and TOPRO3 stained all nuclei (blue). SEMA3A expression increased the fraction of vessels containing apoptotic cells and the apoptotic index of cancer cells (ie, caspase⁺ cells/total cell number) (n=6; **P*<0.05, ****P*<0.001). White arrows point to apoptotic vessels, and green arrows point to apoptotic tumor cells. The images depict representative 4T1-EV and -3A⁺ tumor sections. Scale bars, 20 μ m. B, Tumor vasculature was analyzed in tissue sections as described above by CD31 staining. Both vessel density and relative (%) vessel area were reduced in 66c14 and 4T1 tumors expressing SEMA3A compared with controls (n=6; ***P*<0.01, **P*<0.05). The images depict representative 66c14-EV and 66c14-3A⁺ tumors sections. Scale bars, 50 μ m. C, Tissue sections as described above were costained for endothelial marker CD31 and the pericyte markers α -SMA (upper row) or NG2 (lower row) to assess number of vessels coated with pericytes. Tumor vasculature was remarkably depleted of mural cells in 66c14-3A⁺ and 4T1-3A⁺ compared with controls (n=6, ***P*<0.01, **P*<0.05). The images depict representative 4T1-EV and -3A⁺ tumor sections. Scale bars, 20 μ m.

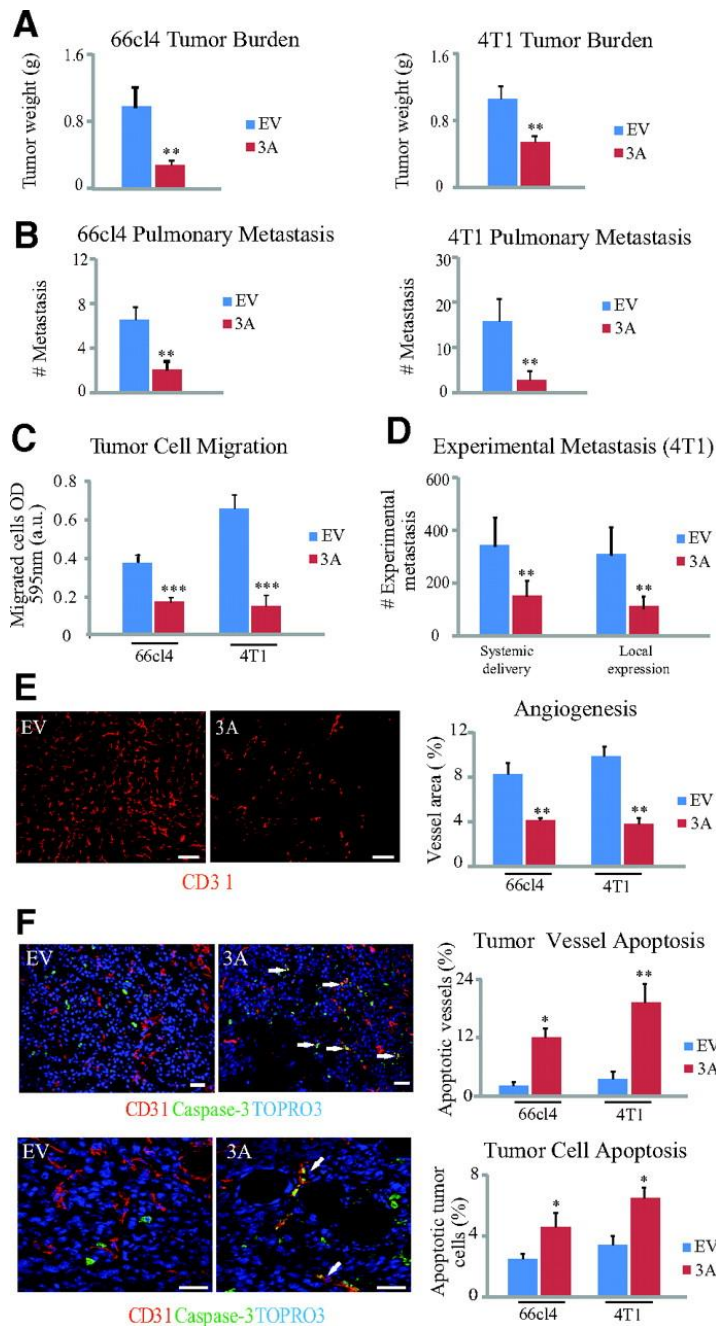


Figure 4.

Systemic delivery of SEMA3A inhibits breast cancer progression and angiogenesis. A and B, Systemic delivery of SEMA3A reduced tumor burden (A) and spontaneous metastatic dissemination to the lungs (B) of 66cl4 and 4T1 cancer cells implanted subcutaneously into syngeneic mice (left and right graphs, respectively) ($n=6$; $**P<0.01$). C, Cancer cell migration was analyzed by Transwell migration assay, in the presence of either SEMA3A-conditioned or a mock medium in the lower chamber. The spontaneous migration of both 66cl4 and 4T1 carcinoma cells was inhibited by SEMA3A; $***P<0.002$. Results are representative of at least 2 independent experiments. D, The metastatic behavior of 4T1 cancer cells was assessed on direct injection in the circulation in the absence of a primary tumor, following by a count of macroscopic metastatic colonies in the lungs 8 days later (experimental metastasis assay; see Methods). Systemic delivery of SEMA3A or local expression of SEMA3A by cancer cells inhibited metastasis formation compared with controls ($n=5$; $**P<0.01$). E and F, Tissue sections of 66cl4 and 4T1 tumors grown in presence of systemic SEMA3A or EV were immunostained for the endothelial cell marker CD31 (red) to visualize blood vessels (E) and for cleaved caspase 3 (green) to visualize apoptotic cells (F). The systemic delivery of SEMA3A reduced vessel area and induced tumor cell and tumor vessel apoptosis ($n=6$; $**P<0.01$, $*P<0.05$). White arrows point to apoptotic vessels. The images depict representative 4T1-EV and -3A⁺ tumor sections (E and lower panel of F), and 66cl4-EV and -3A⁺ tumor sections (upper panel of F). Scale bars, 20 μm (E) and 50 μm (F).

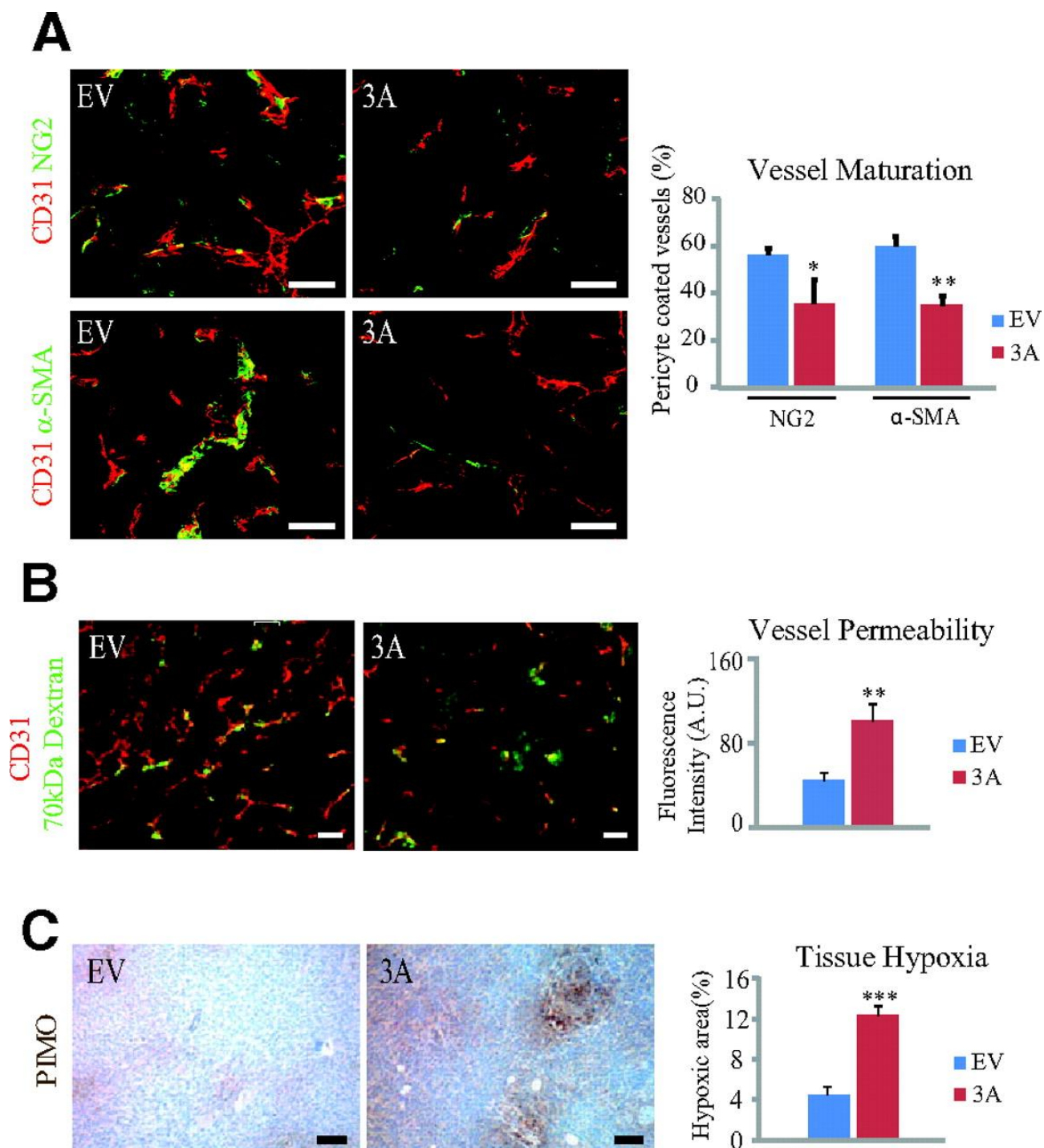


Figure 5.

Systemic delivery of SEMA3A alters vessel functionality. A, Sections from 4T1 tumors with or without systemic delivery of SEMA3A were coimmunostained for the endothelial marker CD31 and the pericyte markers NG2 (upper row) or α -SMA (lower row) to assess vessel structure. Morphometric analysis showed a decrease in pericyte-covered tumor vessels in SEMA3A-treated tumors compared with controls (n=6; * P <0.05, ** P <0.01). Scale bars, 20 μ m. B, Tumor-bearing mice (as described above) were injected with 70-kDa FITC-conjugated dextran to visualize vessel permeability. 4T1 tumor sections grown in sSEMA3A or control EV mice were immunostained for CD31 (red), and FITC-conjugated dextran appears in green. Morphometric analysis revealed increase of extravasated dextran in SEMA3A-treated tumors compared with controls (n=6; ** P <0.01). Scale bars, 50 μ m. C, 4T1 tumor-bearing mice exposed to systemic SEMA3A or EV were injected with pimonidazole (PIMO) to detect hypoxic areas. Immunohistochemistry staining for PIMO (revealed by horseradish peroxidase substrate in brown) showed that systemic SEMA3A increased tumor hypoxic areas compared with controls (n=6; *** P <0.001). Scale bars, 50 μ m.

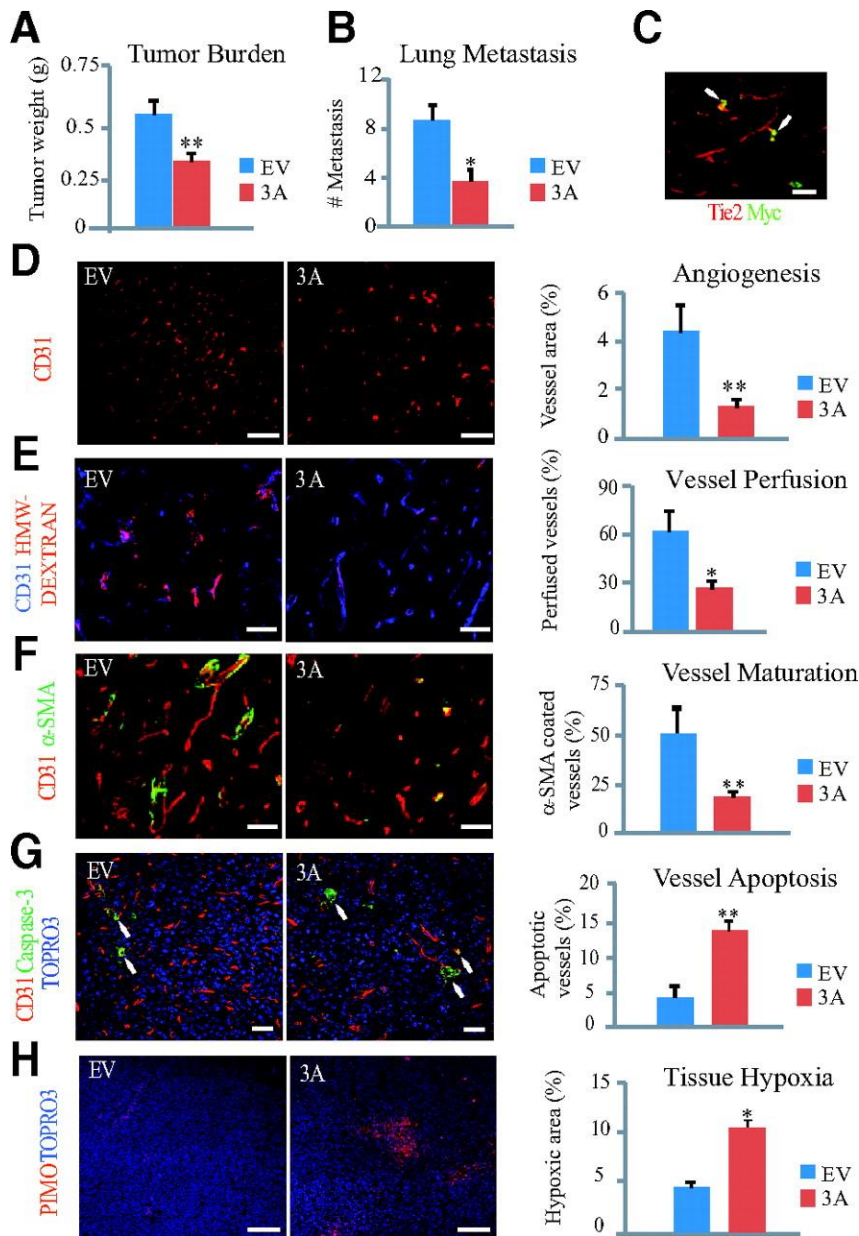


Figure 6.

TEM cell-mediated SEMA3A delivery to the tumor site inhibits tumor progression. A and B, 66cl4 tumor growth in nude mice transplanted with Tie2-3A-transduced bone marrow). TEM cell-mediated delivery of SEMA3A reduced tumor growth (A) and metastatic dissemination (B) ($n=20$; ** $P<0.01$, * $P<0.05$; the graphs display average values \pm SEMs). C, Sections from Tie2-EV and Tie2-3A 66cl4 tumors were coimmunostained to detect Tie2 (red) and myc-tagged SEMA3A (green). Scale bars, 20 μ m. D, Sections from the same tumors as described above were immunostained for CD31 (red) revealed that TEM cell-mediated delivery decreased vessel area compared with controls ($n=12$, ** $P<0.01$; the graphs display average values \pm SEMs). Scale bars, 50 μ m. E, Functional and blood-perfused vessels were labeled by injecting nonpermeable high-molecular weight (2-MDa) tetramethylrhodamine-dextran (red) in tumor-bearing mice (same as described above), as well as staining for CD31 (in blue). TEM cell-mediated delivery of SEMA3A reduced the number of perfused vessels (identified by double staining for CD31 in blue and fluorescent dextran in red ($n=6$ * $P<0.05$). Scale bars, 20 μ m. F, Tumor sections from control and Tie2-3A 66cl4 tumors were coimmunostained for CD31 (red) and the pericyte marker α -SMA (green). Morphometric analysis (second row) showed less pericyte-covered tumor vessels in Tie2-3A tumors compared with controls ($n=12$, ** $P<0.01$; the graphs display average values \pm SEMs). Scale bar, 20 μ m. G, Sections as described above were immunostained for CD31 (red), cleaved-caspase 3 (green), and Topro3 (blue). SEMA3A treated tumors displayed an increase in apoptotic vessels ($n=12$, ** $P<0.01$; the graphs display average values \pm SEMs). White arrows point to apoptotic vessels. Scale bars, 20 μ m. H, Tumors were also immunostained for the hypoxic marker pimonidazole (PIMO; red) and for the nucleic marker Topro3 (blue). Morphometric analysis showed an increase in hypoxia in Tie2-3A tumors compared with controls ($n=6$; * $P<0.05$). Scale bars, 100 μ m.